Journal of Alloys and Compounds 279 (1998) 153–160

Breaking up chains: the nitridocuprates(I) Ba[CuN] $Ba_{16}[(CuN)_8][Cu_2N_3][Cu_3N_4]$ and $Ca_4Ba[CuN_2]_2$

R. Niewa*, F.J. DiSalvo

Department of Chemistry, Cornell University, Ithaca, NY 14853-1301, USA

Received 9 April 1998

Abstract

The three title compounds were prepared from copper or copper(I) oxide and alkaline earth metals in sodium fluxes under medium nitrogen pressures and structurally characterized. Ba[CuN] crystallizes monoclinic in $C\ 2/c$ (No. 15), with $Z=12$, $a=14.462(2)$ Å, $b=5.5700(8)$ Å, $c=9.478(1)$ Å, $\beta=102.960(2)°$. The structure contains infinite chains ${}^1_\infty[CuN^{2-}_{2/2}]$, which are kinked alternately at the first and then the second nitrogen atom. $Ba_{16}[(CuN)_8][Cu_2N_3][Cu_3N_4]$ crystallizes monoclinic in $P2_1/c$ (No. 14), with $Z=1$, $a=9.5611(4)$ Å, $b=7.2731(2)$ Å, $c=13.5225(5)$ Å, $\beta=93.115(2)°$. It is build from infinite helical chains ${}^1_\infty[CuN^{2-}_{2/2}]$ separated by discrete linear $[Cu_2N_3]^{7-}$ and Z-shaped $[Cu_3N_4]^{9-}$ ions. $Ca_4Ba[CuN_2]_2$ crystallizes tetragonal in $P\ 4/ncc$ (No. 130), with $Z=4$, $a=8.2366(4)$ Å, $c=12.5731(6)$ Å. In this compound the nitridocuprate ions are broken down to isolated linear units $[CuN_2]^{5-}$.

Keywords: Ternary Nitrides; Nitridocuprates; Crystal structures

---

1. Introduction

Ternary and higher metal nitrides have attracted a lot of attention over the last decade or so. For transition metal nitrides a wide variety of coordination polyhedra by nitrogen were revealed: octahedral, quadratic pyramidal, quadratic planar, tetrahedral, trigonal planar and linear. In transition metal nitrides linear coordination seems to be limited to late transition metal centers in the oxidation states I or II. The latter oxidation state leads to isolated units $[MN_2]^{4-}$ in $Li_4[FeN_2]$ [1], $Sr_2[MN_2]$ (M=Fe, Ni) [2,3], $AE_2[ZnN_2]$ (AE=Ca, Sr, Ba) [4,5] and $Ba_3[ZnN_2]O$ [6]. Most nitrides with the transition metal in the oxidation state +1 or close to it contain infinite chains ${}^1_\infty[CuN^{2-}_{2/2}]$ which can be linear as in Ca[CuN] [7], Ca[NiN] [8] and $Ca_{1-x}Sr_x[NiN]$ [9], bent to different planar chain conformations in Sr[NiN] [9], Sr[CuN] [7,10], Ba[CoN] [11], Ba[NiN] [12] and $Li_3Sr_3[(NiN)_4]$ [13] or helical in $Ba_8[(NiN)_6]N$ [14].

In lithium nitrides disorder between lithium and cobalt(I), nickel(I) or copper(I) may occur, e.g. in $Li_{3-x}M_xN$ [7,15,16] with the α-Li_3N [17] structure, where the linearly coordinated lithium site is partially substituted by the transition metal atoms, while the trigonal planar coordinated site remains fully occupied by lithium. In quaternary lithium alkaline earth nitrides of the above elements the lithium atoms also can occupy common sites with the transition metal atoms and in this way break up the infinite chains until the smallest isolated units are reached e.g. in the ordered $LiSr_2[CoN_2]$ [18]. Isolated nitridometallate ions are also found in transition metal(I) compounds such as $Sr_{39}[CoN_2]_{12}N_7$ [19] and $Sr_6[CuN_2][Cu_2N_3]$ [10].

Here we report the preparation and the novel structures of Ba[CuN], $Ba_{16}[(CuN)_8][Cu_2N_3][Cu_3N_4]$ and $Ca_4Ba[CuN_2]_2$.

2. Experimental

Due to the moisture sensitivity of most of the materials all work was carried out in a glove box under argon.

$BaN_{0.78}$ was obtained from reaction of barium metal (Aldrich, 99.9%, stoichiometry from weight change during the reaction) with nitrogen of ambient pressure at 800°C. The reaction was carried out in a quartz tube lined with tantalum foil. The nitrogen was purified in a titanium getter at 800°C to remove oxygen impurities.

Ba[CuN] was initially prepared from Cu_2O (Aldrich, 99%), $BaN_{0.78}$ (Cu_2O: Ba=1: 4), NaN_3 (Aldrich, 99%)

---

*Corresponding author.

0925-8388/98/$ – see front matter
PII: S0925-8388(98)00657-4

and sodium (Aldrich, 99.9%). The starting materials were sealed under argon in a niobium tube which was then sealed in vacuum in a quartz tube to prevent oxidation of the niobium. This assembly was heated within 12 h to 800°C, soaked at this temperature for 12 h and then slowly allowed to cool down to room temperature over 100 h. Above about 300°C the sodium azide decomposes to sodium and nitrogen, producing a maximal nitrogen pressure of about 25 bar at 800°C. The sodium apparently serves as flux or reaction medium for the crystal growth. After the reaction the product was recovered from the sodium by extracting with liquid ammonia (Matheson Gas Products, dried and stored over sodium). The product consists of black, well shaped crystals of Ba[CuN], next to barium oxide powder (according to the X-ray powder diffraction pattern, Cu K_α, Scintag XDS 2000). Identical crystals, as shown by their unit cell parameters (Bruker SMART CCD), were produced from fine copper powder and barium under otherwise identical conditions (Cu: Ba= 1:2). But in these reactions unreacted copper always remained in the mixture and the crystal quality was never as good as when Cu_2O was a reactant. Experiments to produce single phase Ba[CuN] from pressed pellets of copper powder and $BaN_{0.78}$ under ambient nitrogen pressure at temperatures between 800°C and 1000°C failed, as observed earlier [7]. Typically the samples lost weight and the multiphase, brass colored solidified melts were mainly composed of unreacted copper and $BaCu_{13}$ [20].

Higher ratios of Ba: Cu of 5:1 in sealed niobium tubes with sodium flux under otherwise the same reaction conditions (elements Cu and Ba) lead to black bulky crystals $Ba_{16}[(CuN)_8][Cu_2N_3][Cu_3N_4]$ next to excess barium nitride. This compound could also be prepared from copper(I) oxide instead of copper.

From mixtures of copper, calcium (Alfa Aesar 99%) and barium (2: 1: 1) $Ca_4Ba[CuN_2]_2$ was obtained next to large amounts of unreacted copper and barium nitride. It crystallizes as black square prisms with sharp 90° or sometimes truncated edges.

Reactions of copper or copper oxide with calcium in sodium to obtain Ca[CuN] single crystals failed. The product mixture was each time composed of copper, calcium nitride and if started from oxides calcium oxide.

Well shaped crystals of each compound were selected under a microscope and sealed in glass capillaries. Diffraction X-ray data sets were collected on a Bruker SMART CCD- diffractometer (Mo $K_{\alpha 1}$, 1321 frames, 30 s exposure time, $\Delta\omega=0.3°$). The unit cells were refined during the integration (program SAINT) based on all strong reflections. An absorption correction was carried out after indexing the crystal faces or using the program SADABS. Structure solution and refinement were carried out using SHELXS-86 [21] and SHELXL-93 [22]. For two crystals of $Ba_{16}[(CuN)_8][Cu_2N_3][Cu_3N_4]$ no reflections indicating a larger unit cell could be found, structure calculations in lower symmetries did not resolve the disorder. Table 1

Table 1
Crystallographic data concerning the structure determinations

Compound	Ba[CuN]	$Ba_{16}[(CuN)_8][Cu_2N_3][Cu_3N_4]$	$Ca_4Ba[CuN_2]_2$
Crystal shape, color	bulky, black	bulky, black	square prism, black
Dimensions/*mm*	0.16×0.08×0.06	0.12×0.10×0.08	0.14×0.13×0.11
Space group, *Z*	*C 2/c* (No. 15), 12	*P 2_1/c* (No. 14), 1	*P 4/ncc*, (No. 130), 4
a/Å	14.462(2)	9.5611(4)	8.2366(4)
b/Å	5.5700(8)	7.2731(2)	
c/Å	9.478(1)	13.5225(5)	12.5731(6)
β/°	102.960(2)	93.115(2)	
Cell volume/$Å^3$	744.1(3)	938.95(8)	852.0(1)
Calculated density/g cm^{-3}	5.755	5.719	3.971
Radiation	Mo Kα	Mo Kα	Mo Kα
Monochromator	Graphite	Graphite	Graphite
Absorption correction	analytical	sadabs	sadabs
Transmission min./max	0.1219/0.3284	0.346/1.000	0.552/1.000
μ/mm^{-1}	0.0418	0.0423	0.0661
$2\theta_{max}$/°	46.54	46.50	46.54
h, k, l	−16 to 11	−10 to 10	−9 to 7
	−6 to 5	−6 to 8	−9 to 8
	−9 to 10	−15 to 13	−13 to 11
Independent reflections	536	1350	312
Reflections with $F_0^2 \geq 2\sigma F_0^2$	514	1168	305
Variables	46	93	28
Goodness of fit (goof)	1.361	1.048	0.806
R_{int}	0.117	0.042	0.037
$R/R_{all}/wR^2$	0.038/0.040/0.101	0.072/0.081/0.197	0.025/0.026/0.068
Extinction parameter	0.0110(7)	0.0044(5)	0.0072(7)
Largest electron difference peak/$Å^{-3}$	1.25	8.91	0.52

Table 2
Atomic coordinates and isotropic displacement parameters (Å^2) for Ba[CuN]

Atom	Site	x	y	z	U_{iso}
Ba(1)	8*f*	0.33098(6)	0.2637(1)	0.37120(8)	0.0083(5)
Ba(2)	4*e*	0	0.2802(2)	$\frac{1}{4}$	0.0083(5)
Cu(1)	8*f*	0.4266(1)	0.2651(3)	0.0606(2)	0.0086(6)
Cu(2)	4*c*	$\frac{1}{4}$	$\frac{1}{4}$	0	0.0075(7)
N(1)	8*f*	0.3416(8)	0.039(2)	0.109(1)	0.012(2)
N(2)	4*a*	0	0	0	0.015(4)

Table 6
Atomic coordinates and isotropic displacement parameters (Å^2) for $Ca_4Ba[CuN_2]_2$

Atom	Site	x	y	z	U_{iso}
Ba	4*c*	$\frac{1}{4}$	$\frac{1}{4}$	0.15455(5)	0.0111(4)
Ca	16*g*	0.0829(1)	0.6310(2)	0.08758(8)	0.0058(4)
Cu	8*f*	0.40360(8)	$-x$	$\frac{1}{4}$	0.0064(4)
N	16*g*	0.5695(6)	0.1242(6)	0.1039(4)	0.006(1)

Table 3
Anisotropic displacement parameters (Å^2) for Ba[CuN]

Atom	U_{11}	U_{22}	U_{33}	U_{23}	U_{13}	U_{12}
Ba(1)	0.0070(7)	0.0110(6)	0.0081(7)	−0.0006(3)	0.0042(3)	0.0001(3)
Ba(2)	0.0073(8)	0.0105(7)	0.0076(7)	0	0.0027(5)	0
Cu(1)	0.005(1)	0.0104(9)	0.012(1)	0.0017(6)	0.0051(7)	−0.0014(6)
Cu(2)	0.003(1)	0.011(1)	0.010(1)	0.0021(8)	0.0034(9)	0.0007(8)
N(1)	0.008(6)	0.011(5)	0.018(6)	0.001(5)	0.008(5)	−0.001(5)
N(2)	0.015(9)	0.014(8)	0.019(8)	−0.002(7)	0.009(7)	0.002(7)

Table 4
Atomic coordinates and isotropic displacement parameters (Å^2) for $Ba_{16}[(CuN)_8][Cu_2N_3][Cu_3N_4]$

Atom	Site	x	y	z	U_{iso}	Occ.
Ba(1)	4*e*	0.0967(2)	0.4785(3)	0.2138(3)	0.067(1)	
Ba(2)	4*e*	0.2490(2)	0.0214(2)	0.1684(1)	0.0149(6)	
Ba(3)	4*e*	0.4107(2)	0.3124(2)	0.4122(1)	0.0116(6)	
Ba(4)	4*e*	0.7677(2)	0.3380(3)	0.0447(1)	0.0325(7)	
N(1)[a]	4*e*	0.029(6)	0.218(9)	0.079(5)	0.04(2)	0.50(2)
N(2)	4*e*	0.152(3)	0.141(4)	0.335(2)	0.029(6)	
N(3)	4*e*	0.332(3)	0.648(4)	0.144(2)	0.021(6)	
N(4)	4*e*	0.497(3)	0.186(3)	0.101(2)	0.016(5)	
Cu(1)	4*e*	0.4218(4)	0.4167(4)	0.1284(3)	0.0143(9)	
Cu(2)	4*e*	0.5849(3)	0.1686(4)	0.2285(2)	0.0116(9)	
Cu(3a)[a]	4*e*	0.0770(8)	0.324(2)	0.4265(6)	0.024(3)	0.50(2)
Cu(3b)[a]	4*e*	0.0869(8)	0.1972(1)	0.4570(6)	0.016(3)	0.50(2)
Cu(4)[a,b]	2*a*	0	0	0	0.021(3)	0.50(2)
N(5)[a,b]	2*a*	0	0	0	0.021(3)	0.50(2)

[a] The occupancies of the sites of N(1), Cu(3b) and Cu(4) were constrained to the same value. The occupancies of the sites of N(5) and Cu(3a) also were constrained to the same value, while the sum over both occupancies was constrained to one.

[b] The displacement parameters of Cu(4) and N(5) were constrained to the same values, since both atoms are disordered over an identical crystallographic site.

Table 5
Anisotropic displacement parameters (Å^2) for $Ba_{16}[(CuN)_8][Cu_2N_3][Cu_3N_4]$

Atom	U_{11}	U_{22}	U_{33}	U_{23}	U_{13}	U_{12}
Ba(1)	0.015(1)	0.027(1)	0.156(3)	0.054(2)	−0.021(1)	−0.0080(9)
Ba(2)	0.023(1)	0.004(1)	0.018(1)	−0.0003(7)	0.0054(7)	0.0007(7)
Ba(3)	0.016(1)	0.008(1)	0.011(1)	0.0024(6)	−0.0052(7)	0.0004(6)
Ba(4)	0.020(1)	0.063(2)	0.014(1)	−0.012(1)	−0.0063(8)	−0.007(1)
Cu(1)	0.018(2)	0.005(2)	0.019(2)	−0.003(1)	−0.004(2)	0.001(1)
Cu(2)	0.017(2)	0.007(2)	0.010(2)	0.000(1)	−0.006(1)	0.000(1)
Cu(3a)	0.015(4)	0.035(8)	0.021(5)	−0.015(5)	−0.004(3)	−0.003(4)
Cu(3b)	0.018(4)	0.012(6)	0.018(4)	−0.004(4)	−0.002(3)	0.002(3)
Cu(4)/N(5)[a]	0.028(5)	0.017(5)	0.018(5)	0.004(4)	−0.006(4)	−0.007(4)

[a] The displacement parameters of Cu(4) and N(5) were constrained to the same values, since both atoms are disordered over an identical crystallographic site.

Table 7
Anisotropic displacement parameters (Å^2) for $Ca_4Ba[CuN_2]_2$

Atom	U_{11}	U_{22}	U_{33}	U_{23}	U_{13}	U_{12}
Ba	0.0075(4)	0.0075(4)	0.0183(6)	0	0	0
Ca	0.0060(7)	0.0052(7)	0.0062(7)	0.0001(4)	−0.0002(4)	−0.0011(5)
Cu	0.0076(5)	0.0076(5)	0.0040(6)	−0.0001(3)	−0.0001(3)	−0.0004(4)
N	0.004(2)	0.009(3)	0.006(2)	−0.001(2)	−0.002(2)	−0.001(2)

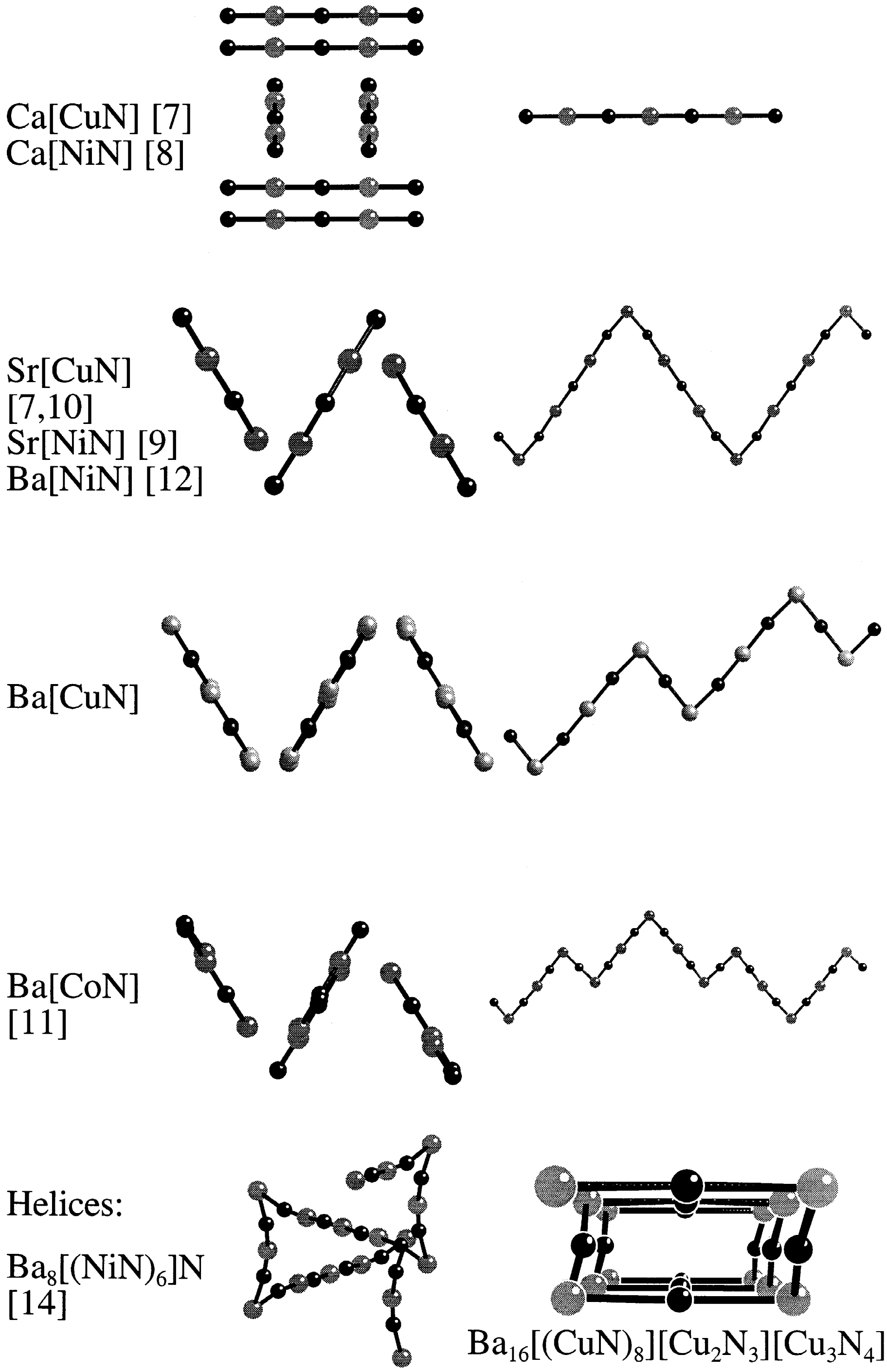

Fig. 1. Comparison of chain conformations and interchain orientations in cobalt(I), nickel(I) and copper(I) ternary nitrides containing infinite chains.

gives further information on the data collections and refinements. Tables 2–7 include positional and displacement parameters.

3. Structure descriptions and discussion

The structure of Ba[CuN] is built of infinite chains $^1_\infty[\mathrm{CuN}^{2-}_{2/2}]$, bent alternately at the first and then the second nitrogen atom. These chains are packed parallel to each other in a herringbone pattern. Fig. 1 gives an overview of the known chain conformations and relative orientations in the nitrides of this type. In Ba[CuN] the copper and N(2) atoms in the chain are linearly coordinated by each other, with bond angles close to or by symmetry 180°, while N(1) shows a bond angle of $\sphericalangle$(Cu–N(1)–Cu)≈90°. More detailed data on bond lengths and angles are summarized in Fig. 2 and Table 8.

Table 8
Selected bond lengths (Å) and angles (deg) in Ba[CuN]

Ba(1)–N(1)	2.79(1)	Cu(1) –N(2)	1.856(2)
Ba(1)–N(2)	2.803(1)	Cu(1) –N(1)	1.89(1)
Ba(1)–N(1)	2.82(1)	Cu(1) –Cu(2)	2.490(2)
Ba(1)–N(1)	2.97(1)		
		Cu(2) –N(1) 2x	1.89(1)
Ba(2)–N(1) 2x	2.78(1)	Cu(2) –Cu(1) 2x	2.490(2)
Ba(2)–N(2) 2x	2.837(8)		
		N(1) –Cu(1) –N(2)	174.3(3)
		N(1) –Cu(2) –N(1)	180
Ba–Cu≥	3.285(2)	Cu(1) –N(1) –Cu(2)	82.4(4)
Ba–Ba≥	3.747(2)	Cu(1) –N(2) –Cu(1)	180

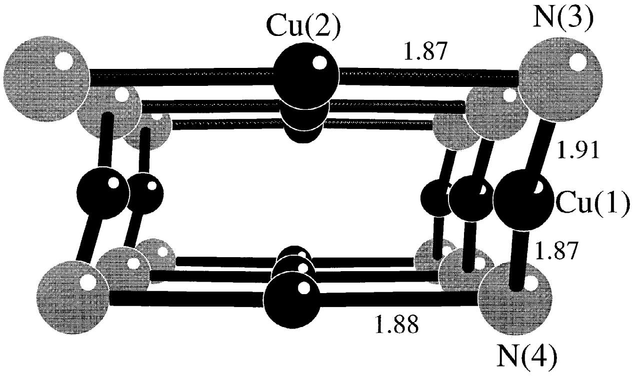

Fig. 3. A view of the helix $^1_\infty[\mathrm{CuN}^{2-}_{2/2}]$ in $\mathrm{Ba_{16}[(CuN)_8][Cu_2N_3][Cu_3N_4]}$. Distances are given in Å.

With a larger ratio of barium to copper in the reaction mixture the isolated ions $[\mathrm{Cu_2N_3}]^{7-}$ and $[\mathrm{Cu_3N_4}]^{9-}$ are formed. They co-crystallize together with infinite helices $^1_\infty[\mathrm{CuN}^{2-}_{2/2}]$ in the structure of $\mathrm{Ba_{16}[(CuN)_8][Cu_2N_3][Cu_3N_4]}$. The latter helix is depicted in Fig. 3. It is bent at every nitrogen atom with bond angles $\sphericalangle$(Cu–N–Cu) close to 90°. Neighboring helices have opposite rotation directions. Layers of helices are separated by layers of the previously mentioned isolated units $[\mathrm{Cu_2N_3}]^{7-}$ and $[\mathrm{Cu_3N_4}]^{9-}$ as shown in Fig. 4. $[\mathrm{Cu_2N_3}]^{7-}$ is nearly linear with bond angles at copper and nitrogen larger than 174°. The ion $[\mathrm{Cu_3N_4}]^{9-}$ in contrast is kinked at both bridging nitrogen atoms with an angle of about 80°. Both ions randomly occupy the same position in the structure at 50% probability, so that the terminal nitrogen atoms N(2) of both ions occupy exactly the same crystallographic position. Additionally, the central copper atom of the bent $[\mathrm{Cu_3N_4}]^{9-}$ ion Cu(4) and the central nitrogen atom N(5) of the linear $[\mathrm{Cu_2N_3}]^{7-}$ unit are located on the same special site. To clarify these relations Fig. 5 shows both ions, together with the disorder model used to refine the data. The half occupancy of this position by both different ions is the result of an unconstrained refinement of the diffraction data, as well as of the final constrained refinement we are reporting here. Additionally it follows from the charge balance condition for the compound; since sixteen $\mathrm{Ba^{2+}}$ ions and eight units of the helix $^1_\infty[\mathrm{CuN}^{2-}_{2/2}]$ per unit cell require sixteen further negative charges. This condition is satisfied by one

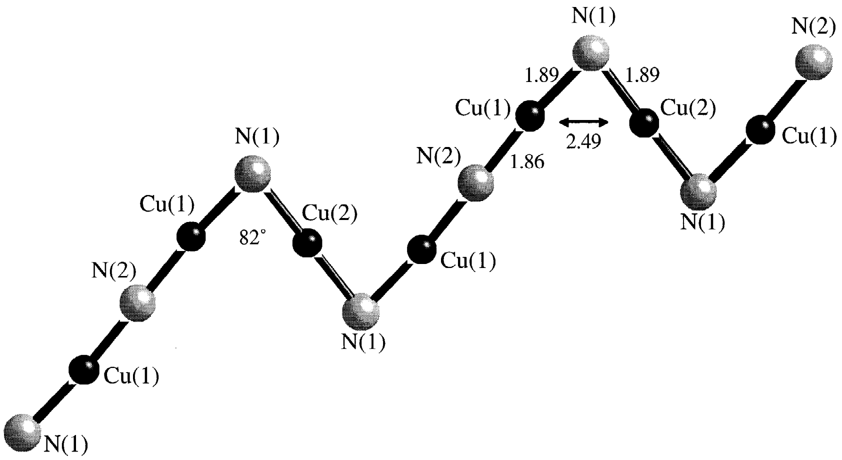

Fig. 2. A segment of the chain $^1_\infty[\mathrm{CuN}^{2-}_{2/2}]$ in Ba[CuN]. Distances are given in Å.

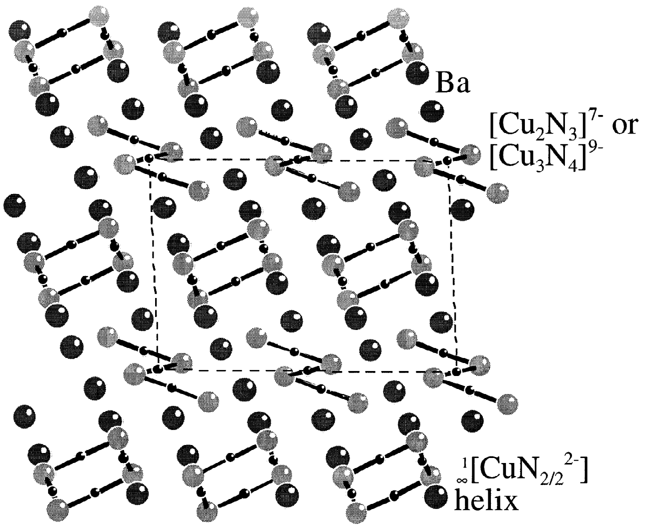

Fig. 4. A segment of the structure of $Ba_{16}[(CuN)_8][Cu_2N_3][Cu_3N_4]$ viewed down the b-axis. Only the helical chains $^1_\infty[CuN^{2-}_{2/2}]$, the Z-shaped $[Cu_3N_4]^{9-}$ ions and the barium ions are shown. The linear $[Cu_2N_3]^{7-}$ ions are omitted for clarity.

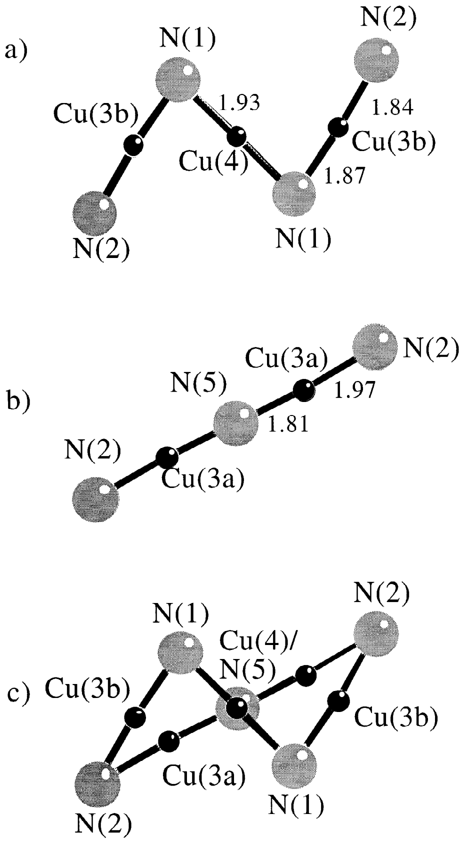

Fig. 5. (a) Z-shaped ion $[Cu_3N_4]^{9-}$ in $Ba_{16}[(CuN)_8][Cu_2N_3][Cu_3N_4]$. (b) linear ion $[Cu_2N_3]^{7-}$ in $Ba_{16}[(CuN)_8][Cu_2N_3][Cu_3N_4]$. (c) Formal superimposed disordered ions $[Cu_2N_3]^{7-}$ and $[Cu_3N_4]^{9-}$ in $Ba_{16}[(CuN)_8][Cu_2N_3][Cu_3N_4]$. The terminal nitrogen atoms N(2) of both units occupy the same crystallographic position. The special position in the center of both ions is either occupied by an Cu(4) or an N(5) atom.

$[Cu_2N_3]^{7-}$ ion and one $[Cu_3N_4]^{9-}$ ion per unit cell. The large anisotropic displacement parameters of Ba(1) and Ba(4) are a direct result of the disorder. Both barium atoms are coordinated by N(1), a position that is only occupied if a $[Cu_3N_4]^{9-}$ ion is in the neighborhood of the barium atoms in question. In contrast the normally behaved Ba(3) has no N(1) atom in its first coordination sphere, while Ba(2) has a medium distance to the N(5) position, which is alternatively occupied if N(2) is empty. Table 9 gives more detailed information on bond distances and angles.

$Ca_4Ba[CuN_2]_2$ crystallizes in the unusual space group *P 4/ncc*. In the structure the nitridocuprate ions are completely broken apart into isolated linear dumbbells $[CuN_2]^{5-}$. These are stacked together with the alkaline earth ions within layers (Fig. 6). Distances and angles can be found in Table 10.

In all three compounds bridging nitrogen atoms are coordinated by four alkaline earth atoms in addition to the two copper atoms, terminal nitrogen atoms have one copper and five alkaline earth neighbors. This leads to a distorted octahedral environment which seems to be the preferred surrounding of nitrogen in ternary nitrides. Calcium atoms and the large barium atoms are only tetrahedrally coordinated by nitrogen atoms. Deviations from these coordinations in $Ba_{16}[(CuN)_8][Cu_2N_3][Cu_3N_4]$ are the result of the disorder of the isolated nitridocuprate ions.

In all known nitridocuprates with condensed anions the

Table 9
Selected bond lengths (Å) and angles (deg) in $Ba_{16}[(CuN)_8][Cu_2N_3][Cu_3N_4]$

Ba(1)–N(1)	2.68(6)	helix:	
Ba(1)–N(2)	2.70(3)	Cu(1)–N(4)	1.87(2)
Ba(1)–N(3)	2.77(3)	Cu(1)–N(3)	1.91(3)
Ba(1)–N(2)	2.99(3)	Cu(2)–N(3)	1.87(3)
		Cu(2)–N(4)	1.88(2)
Ba(2)–N(2)	2.64(3)	Cu(1)–Cu(2)	2.668(5)
Ba(2)–N(1)	2.77(6)	Cu(1)–Cu(2)	2.700(4)
Ba(2)–N(4)	2.85(2)	N(3)–Cu(1)–N(4)	174(1)
Ba(2)–N(3)	2.85(3)	N(3)–Cu(2)–N(4)	179(1)
Ba(2)–N(5)	3.208(2)	Cu(1)–N(3)–Cu(2)	90(1)
		Cu(1)–N(4)–Cu(2)	92(1)
Ba(3)–N(4)	2.65(2)		
Ba(3)–N(4)	2.87(2)	$[Cu_2N_3]^{7-}$:	
Ba(3)–N(3)	2.88(2)	Cu(3a)–N(5)	1.805(9)
Ba(3)–N(2)	2.91(3)	Cu(3a)–N(2)	1.97(3)
		N(2)–Cu(3a)–N(5)	175(1)
Ba(4)–N(1)	2.66(6)	Cu(3a)–N(5)–Cu(3a)	180
Ba(4)–N(3)	2.68(3)		
Ba(4)–N(2)	2.82(3)	$[Cu_3N_4]^{9-}$:	
Ba(4)–N(4)	2.95(2)	Cu(3b)–N(2)	1.83(3)
		Cu(3b)–N(1)	1.87(6)
		Cu(4)–N(1) 2x	1.93(6)
		Cu(3b)–Cu(4) 2x	2.435(9)
		N(1)–Cu(3b)–N(2)	174(2)
Ba–Cu≥	2.96(1)	N(1)–Cu(4)–N(1)	180
Ba–Ba≥	3.694(3)	Cu(3b)–N(1)–Cu(4)	80(2)

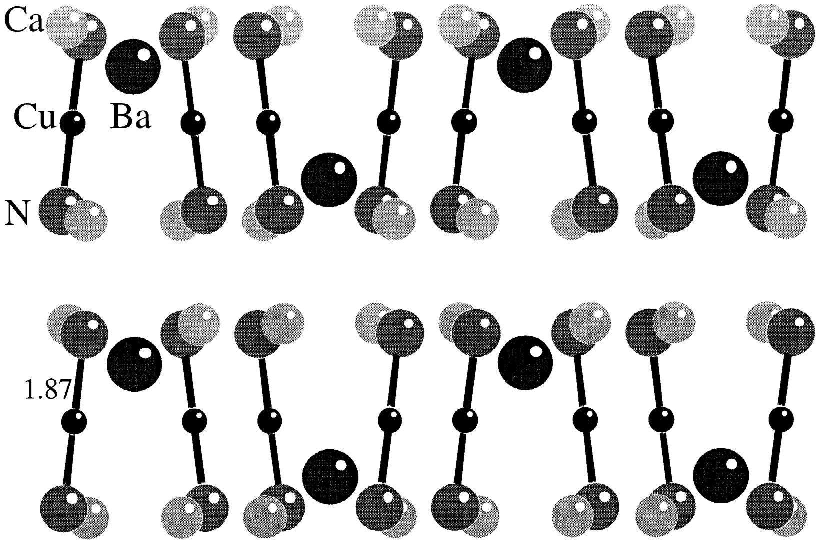

Fig. 6. The arrangement of $[CuN_2]^{5-}$, calcium and barium ions in the structure of $Ca_4Ba[CuN_2]_2$.

bond angles around bridging nitrogen atoms are either close to 90° or 180°. In the former case Cu(I)–Cu(I) distances as short as 2.44 Å can be reached; distances considerably shorter than in copper metal (2.56 Å), for which in the past d^{10}–d^{10} bonding interactions were discussed. Virtually the same distances between transition metal atoms (2.37 Å–2.48 Å) were found in the analogues Ba[CoN] (d^8) [11], Sr[NiN] [9] and Ba[NiN] (d^9) [12]. For the latter nickel–nickel bonding interactions are demonstrated by the small magnetic moment of 1.0 μ_B and a chain with $\frac{1}{3}$ of the nickel atoms with no near nickel neighbor. The other related compounds show temperature independent paramagnetism as far as the magnetic behavior was studied. Except for Sr[CuN] [7,10], Sr[NiN] [9] and Ba[NiN] [12] the compounds with kinked chains have chain conformations, in which every transition metal center has at least one transition metal neighbor at a short distance within the chain.

The complex nitridocuprate anions of the ternary copper nitrides can be understood as segments of the copper nitride structure. Cu_3N crystallizes in a anti-ReO_3 structure with Cu(I) in linear coordination by nitrogen atoms [23]. The nitrogen atoms are octahedrally surrounded by six copper atoms. Ca[CuN] [7], Sr[CuN] [7,10] and Ba[CuN] contain infinite chains $^{1}_{\infty}[CuN^{2-}_{2/2}]$ within copper in almost linear coordination by nitrogen, while the bond angle at nitrogen is either about 90° or 180°. With a higher content of electropositive metal the chains are broken up into isolated dumbbells $[CuN_2]^{5-}$ and V-shaped $[Cu_2N_3]^{7-}$ ions in $Sr_6[CuN_2][Cu_2N_3]$ [10] or linear $[Cu_2N_3]^{7-}$ and Z-shaped $[Cu_3N_4]^{9-}$ ions in $Ba_{16}[(CuN)_8]$-$[Cu_2N_3][Cu_3N_4]$. The helices in the latter compound can be imagined as formed from a cyclic $[Cu_4N_4]$ (as known from oxides as $[Cu_4O_4]^{4-}$ [24]) by breaking one bond, stretching and extending to the next $[Cu_4N_4]$ unit. Table 11 compares the known copper nitrides without disorder in the structure with some copper(I) oxide examples. The large increase in the copper–nitrogen bond lengths in $CuTaN_2$ [25] can be understood as result of the stronger covalent tantalum–nitrogen interactions compared to the alkaline earth metal–nitrogen bonds.

The formation of Ba[CuN] from oxygen containing starting materials is somewhat surprising. Reactions of transition metal oxides to nitrides often yield either oxonitridometallates or nitridometallate oxides. Oxonitridometallates are normally formed if the heavier alkali metals sodium to cesium or barium are serving as the electropositive elements, e.g. in $Na_4[WN_2O_2]$ [26] and $K_6[Mo_2N_4O_3]$ [27]. For lithium or alkaline earth metal nitrides mostly nitridometallate oxides were reported, e.g. $Ba_3[ZnN_2]O$ [6] or $Li_{16}[TaN_4]_2O$ [28]. Only the ammonolysis reactions of Li_2MO_4 (M = Mo, W) [29,30] and transition metal oxides like $M'MO_4$ (M′ = Cr, Mn, Fe, Co, Ni, M = Mo, W) e.g. [31–33] are reported to produce oxygen free ternary nitrides.

Table 10
Selected bond lengths (Å) and angles (deg) in $Ca_4Ba[CuN_2]_2$

Ba–N	4x	2.899(5)	Cu–N	2x	1.865(5)
			N–Cu–N		179.7(3)
Ca–N		2.410(5)			
		2.457(5)	Ba–Cu≥		3.3439(6)
		2.473(5)	Ba–Ca≥		3.528(1)
		2.499(5)	Ca–Ca≥		3.249(2)
			Ca–Cu≥		3.037(1)

Acknowledgements

This work was partially founded by the National Science Foundation through Research Grant DMR-9508522 and by

Table 11
Comparison of structural features and bond distances in copper(I) nitrides and analogues oxides

		Oxide examples		$\bar{d}$(Cu–O)/Å	Nitride examples		$\bar{d}$(Cu–N)/Å
Three-dimensional networks		Cu_2O [34]	${}^{3}_{\infty}[\mathrm{CuO}_{2/4}]$	1.84	Cu_3N [23]	${}^{3}_{\infty}[\mathrm{CuN}_{2/6}]$	1.91
					Cu_3PdN [39]		1.93
Infinite chains	linear				Ca[CuN] [7]	${}^{1}_{\infty}[\mathrm{CuN}^{2-}_{2/2}]$	1.86
	zigzag	$Sr[Cu_2O_2]$ [35]	${}^{1}_{\infty}[\mathrm{CuO}^{-}_{2/2}]$	1.84	Sr[CuN] [7,10]	${}^{1}_{\infty}[\mathrm{CuN}^{2-}_{2/2}]$	1.87
		$Ba[Cu_2O_2]$ [36]		1.84	Ba[CuN]		1.87
Infinite chains and isolated units	helical, Z-shaped and linear				$Ba_{16}[(CuN)_8]$	${}^{1}_{\infty}[\mathrm{CuN}^{2-}_{2/2}]$	1.88
					$[Cu_2N_3][Cu_3N_4]$	${}^{0}[\mathrm{Cu}_3\mathrm{N}_4]^{9-}$	1.88
						${}^{0}[\mathrm{Cu}_2\mathrm{N}_3]^{7-}$	1.89
Isolated units	four-ring	K[CuO] [24]	${}^{0}[(\mathrm{CuO}_{2/2})_4]^{4-}$	1.84			
	dumb-bell and V-shaped				$Sr_6[CuN_2][Cu_2N_3]$ [10]	${}^{0}[\mathrm{CuN}_2]^{5-}$	1.86
						${}^{0}[\mathrm{Cu}_2\mathrm{N}_3]^{7-}$	1.90
	dumb-bell	$La[CuO_2]$ [37]	${}^{0}[\mathrm{CuO}_2]^{3-}$	1.84	$Ca_4Ba[CuN_2]_2$	${}^{0}[\mathrm{CuN}_2]^{5-}$	1.87
		$Cu_2Ta_4O_{11}$ [38]		1.93	$CuTaN_2$ [25]		2.08

the NEDO foundation. R. N. thanks the Deutsche Forschungsgemeinschaft for providing a Forschungsstipendium.

References

[1] A. Gudat, R. Kniep, A. Rabenau, Angew. Chem. Int. Ed. Engl. 30 (1991) 199.
[2] P. Höhn, R. Kniep, Z. Naturforsch. 47b (1992) 477.
[3] G.R. Kowach, PhD Thesis, Cornell University, 1997.
[4] M.Y. Chern, F.J. DiSalvo, J. Solid State Chem. 88 (1990) 528.
[5] H. Yamane, F.J. DiSalvo, J. Solid State Chem. 119 (1995) 375.
[6] H. Yamane, F.J. DiSalvo, J. Alloys Comp. 234 (1996) 203.
[7] J. Jäger, PhD Thesis, Technische Hochschule Darmstadt, 1995.
[8] M.Y. Chern, F.J. DiSalvo, J. Solid State Chem. 88 (1990) 459.
[9] T. Yamamoto, S. Kikkawa, F. Kanamaru, J. Solid State Chem. 115 (1995) 353.
[10] F.J. DiSalvo, S.S. Trail, H. Yamane, N.E. Brese, J. Alloys Comp. 255 (1997) 122.
[11] A. Tennstedt, R. Kniep, Z. Anorg. Allg. Chem. 620 (1994) 1781.
[12] A. Gudat, S. Haag, R. Kniep, A. Rabenau, J. Less-Common Met. 159 (1990) L29.
[13] A. Gudat, R. Kniep, A. Rabenau, Z. Anorg. Allg. Chem. 597 (1991) 61.
[14] A. Gudat, W. Milius, S. Haag, R. Kniep, A. Rabenau, J. Less-Common Met. 168 (1991) 305.
[15] W. Sachsze, R. Juza, Z. Anorg. Allg. Chem. 259 (1949) 278.
[16] A. Gudat, R. Kniep, A. Rabenau, Thermochimica Acta 160 (1990) 49.
[17] A. Rabenau, H. Schulz, J. Less-Common Met. 50 (1976) 155.
[18] P. Höhn, R. Kniep, Z. Naturforsch. 47b (1992) 434.
[19] G.R. Kowach, H.Y. Lin, F.J. DiSalvo, J. Solid State Chem. in press.
[20] P.B. Braun, J.L. Meijerling, Recl. Trav. Chim. Pays-Bas 78 (1959) 71.
[21] G.M. Sheldrick, G. Krüger, R. Goddard, SHELXS-86, Crystallographic Computing, Oxford University Press, Oxford, 1985.
[22] G.M. Sheldrick, SHELXL-93 Crystal Structure Refinement-MS DOS 32-Bit Version, Institut für Anorganische Chemie der Universität Göttingen, 1993.
[23] U. Zachwieja, H. Jacobs, J. Less-Common Met. 161 (1990) 175.
[24] W. Losert, R. Hoppe, Z. Anorg. Allg. Chem. 524 (1985) 7.
[25] U. Zachwieja, H. Jacobs, Eur. J. Solid State Inorg. Chem. 28 (1991) 1055.
[26] D. Ostermann, H. Jacobs, B. Harbrecht, Z. Anorg. Allg. Chem. 619 (1993) 1277.
[27] R. Niewa, H. Jacobs, J. Alloys Comp. 217 (1995) 38.
[28] Ch. Wachsmann, Th. Brokamp, H. Jacobs, J. Alloys Comp. 185 (1992) 109.
[29] S.H. Elder, L.H. Doerrer, F.J. DiSalvo, J.B. Parise, D. Guyomard, J.M. Tarascon, Chem. Mater. 4 (1992) 928.
[30] P. Subramanya Herle, M.S. Hegde, N.Y. Vasanthacharya, J. Gopalakrishnan, G.N. Subbanna, J. Solid State Chem. 112 (1994) 208.
[31] P. Subramanya Herle, N.Y. Vasanthacharya, M.S. Hegde, J. Gopalakrishnan, J. Alloys Comp. 217 (1995) 22.
[32] D.S. Bem, H.-C. zur Loye, J. Solid State Chem. 104 (1993) 467.
[33] K.S. Weil, P.N. Kumta, J. Solid State Chem. 128 (1997) 185.
[34] M.C. Neuburger, Z. Phys. 67 (1931) 845.
[35] Chr.L. Teske, Hk. Muller-Buschcaum, Z. Anorg. Allg. Chem. 379 (1970) 113.
[36] C.L. Teske, H. Müller-Buschbaum, Z. Naturforsch. 27b (1972) 296.
[37] H. Haas, E. Kordes, Z. Kristallogr. 129 (1969) 259.
[38] L. Jahnberg, M. Sundberg, J. Solid State Chem. 100 (1992) 212.
[39] H. Jacobs, U. Zachwieja, J. Less-Common Met. 170 (1991) 185.